

Research Paper

# Aplnra/b Sequentially Regulate Organ Left-Right Patterning via Distinct Mechanisms

Chengke Zhu<sup>1,3\*</sup>, Zhenghua Guo<sup>4\*</sup>, Yu Zhang<sup>2\*</sup>, Min Liu<sup>2</sup>, Bingyu Chen<sup>2</sup>, Kang Cao<sup>2</sup>, Yongmei Wu<sup>2</sup>, Min Yang<sup>2</sup>, Wenqing Yin<sup>7</sup>, Haixia Zhao<sup>2</sup>, Haoran Tai<sup>2</sup>, Yu Ou<sup>5</sup>, Xiaoping Yu<sup>5</sup>, Chi Liu<sup>6</sup>, Shurong Li<sup>2</sup>, Bingyin Su<sup>2</sup>, Yi Feng<sup>3</sup>, Sizhou Huang<sup>2</sup>✉

1. College of Animal Science in Rongchang Campus, Southwest University, Key Laboratory of Freshwater Fish Reproduction and Development, Ministry of Education, Key Laboratory of Aquatics Science of Chongqing, Chongqing 402460, China.
2. Development and Regeneration Key Laboratory of Sichuan Province, Department of Anatomy and Histology and Embryology, Chengdu Medical College, Chengdu 610500, China.
3. UoE Centre for Inflammation Research, Queen's Medical Research Institute, University of Edinburgh, Edinburgh Bioquarter, 47 Little France Crescent, Edinburgh, EH16 4TJ, UK.
4. Ministry of Education Key Laboratory of Child Development and Disorders; Key Laboratory of Pediatrics in Chongqing, CSTC2009CA5002; Chongqing International Science and Technology Cooperation Center for Child Development and Disorders, Children's Hospital of Chongqing Medical University, 400014, Chongqing, China.
5. School of Public Health, Chengdu Medical College, Chengdu 610500, China
6. Department of Nephrology, Institute of Nephrology of Chongqing and Kidney Center of PLA, Xinqiao Hospital, Third Military Medical University, Chongqing, PR China.
7. Renal Division, Brigham and Women's Hospital, Department of Medicine, Harvard Medical School, Boston, Massachusetts. USA.

\*These authors contributed equally to this work.

✉ Corresponding author: Sizhou Huang, Email: huangyuy1027@cmc.edu.cn; Tel: (086) 28-6273-9327; Fax: (086)28-62739298.

© Ivyspring International Publisher. This is an open access article distributed under the terms of the Creative Commons Attribution (CC BY-NC) license (<https://creativecommons.org/licenses/by-nc/4.0/>). See <http://ivyspring.com/terms> for full terms and conditions.

Received: 2018.09.20; Accepted: 2019.03.12; Published: 2019.05.11

## Abstract

The G protein-coupled receptor APJ/Aplnr has been widely reported to be involved in heart and vascular development and disease, but whether it contributes to organ left-right patterning is largely unknown. Here, we show that in zebrafish, *aplnr/b* coordinates organ LR patterning in an *apela/apln* ligand-dependent manner using distinct mechanisms at different stages. During gastrulation and early somitogenesis, *aplnr/b* loss of function results in heart and liver LR asymmetry defects, accompanied by disturbed KV/cilia morphogenesis and disrupted left-sided *Nodal/spaw* expression in the LPM. In this process, only *aplnr/a* loss of function results in KV/cilia morphogenesis defect. In addition, only *apela* works as the early endogenous ligand to regulate KV morphogenesis, which then contributes to left-sided *Nodal/spaw* expression and subsequent organ LR patterning. The *aplnr/a-apela* cascade regulates KV morphogenesis by enhancing the expression of *foxj1a*, but not *fgf8* or *dnh9*, during KV development. At the late somite stage, both *aplnr/a* and *aplnr/b* contribute to the expression of *lft1* in the trunk midline but do not regulate KV formation, and this role is possibly mediated by both endogenous ligands, *apela* and *apln*. In conclusion, our study is the first to identify a role for *aplnr/b* and their endogenous ligands *apela/apln* in LR patterning, and it clarifies the distinct roles of *aplnr/a-apela* and *aplnr/b-apela/apln* in orchestrating organ LR patterning.

Key words: *aplnr/b*, *apela/apln*, left right patterning, *spaw*, midline

## Introduction

G protein-coupled receptor (GPCR) APJ, being close to the angiotensin II (Ang II) receptor, was identified as an orphan GPCR [1]. It remained an orphan receptor until a 36-amino acid peptide apelin was discovered [2]. In cardiac development and disease, the function of apelin-APJ has been studied in

many cases [3-6]. In apelin and APJ knockout (KO) mice, the sarcomeres of cardiomyocytes are impaired in isolated ventricular myocytes [3]. Apelin/APJ also shows a role in the sustainability and amplification of the cardiac response to stress [5] and in essential hypertension (EHT) [6]. Apelin-APJ plays a role in the

Cripto signaling pathway in mammalian cardiac myogenesis by extracellular signal-regulated kinase/p70S6 kinase [7]. In vascular diseases, the upregulation of apelin in the atherosclerosis of human coronary artery suggested apelin-APJ signaling contributes to coronary vasospasm [8], while conflicting evidence in KO studies has shown antagonistic and inducing roles of apelin-APJ signaling in atherosclerotic formation [9, 10]. All these data indicate that the role of apelin/APJ and its mechanism of action in mammals need to be clarified.

The zebrafish homologs of APJ, *aplnra/b* and their endogenous ligands *apela/apln* were identified recently [11-14]. *Aplnra/b* is involved in regulating gastrulation cell movement [14, 15] and heart [13, 16-18] and vasculature development [19-21], which motivated the study for *aplnra/b* and its ligands *apela/apln* in disease and embryonic development. In the zebrafish *grinch* (*grn*) mutant, *aplnrb* loss of function leads to a reduced myocardial progenitor cells (MPCs) via cell-autonomous way [13, 18]. *Aplnra/b* directly modulates Nodal/TGF $\beta$  signaling to determine heart progenitor cells in a another cell-non-autonomous fashion during gastrulation [16], as well as regulating progenitor movement through a G-protein signaling-independent manner in later stages [17]. Detailed analyses showed that overexpression of *apln*, though not loss of function, phenocopied the heart development defect of the *grinch* (*grn*)/or *apela* mutant [12, 13, 18]. These findings suggested that *apln*, *apela* and their receptor *aplnra/b* might play different roles in heart development, as well as the possibility that another receptor may exist. The ligand Apela but not the receptor Aplinr is expressed in human embryonic stem cells [12], suggesting the distinct roles of *apln*, *apela* and receptor *aplnra/b* in heart or other organ development. All these reports have shown the association between *aplnr* and the underlying complicated mechanisms during heart development. However, the role of *aplnr* in cardiovascular development is still not clear.

Left-right (LR) patterning is a fundamental process in early development, and most of its mechanisms are conserved in the animal kingdom [22,23]. In zebrafish, left-sided *Nodal/Spaw* in the lateral plate mesoderm (LPM) [24] is initiated and amplified by the Node flow in Kupffer's vesicle (KV), which sequentially regulates organ LR patterning [25-29]. In addition to the central role of KV/cilia (or Node/cilia in mouse) in initiating asymmetric *Nodal/Spaw*, *pegasus*, *nek8* and *atp1a1a.1* regulate left-sided *Nodal/Spaw* expression pattern in a KV/cilia-independent manner [30-32], suggesting that the procedure of initiating and maintaining

asymmetric *Nodal/Spaw* is intricate.

In zebrafish, *aplnra/b* are zygotic genes and are expressed after blastula stage [11, 18]. At the early gastrulation stage, *aplnra* loss of function leads to gastrulation movement defect [15] and heart progenitor decreasing [12, 13, 18]. More recently, *apela* was discovered to work as the ligand for *aplnra/b* to guide vascular precursors migrate to the midline [33]. During gastrulation, *aplnra* but not *aplnrb* is expressed in the cells near dorsal forerunner cells (DFCs) and in DFCs (Fig. S1), the progenitors of KV. At the somite stage, *aplnra/b* were expressed in the cells near the midline (Fig. S1 and [33]). Since the roles of DFCs/KV and the midline in LR asymmetry patterning are widely reported [24, 26, 28, 29], we hypothesized that *aplnra/b* might play a crucial role in LR asymmetry patterning. Here, we found that *aplnra/b* were involved in organ LR patterning via the ligands *apela/apln* at different developmental stages.

## Results

### The complementary roles of *aplnra/b* in organ LR asymmetry patterning

The *aplnra/b* expression pattern and the critical role in gastrulation cell movement [11, 14] led us to hypothesize *aplnra/b* play vital roles in LR patterning. To examine this hypothesis, we synthesized the antisense morpholino oligos for zebrafish *aplnra/b* (MO<sup>ATG</sup>, Gene tools) to block the translation of *aplnra/b* [13, 18]. Since *aplnrb* loss of function leads to heart progenitors disappearing or decreasing greatly [13, 18] (Fig. S2 C), which inhibits the analysis of heart LR patterning in *aplnrb* morphants, we first examined the heart LR patterning in *aplnra* morphants to evaluate the role of *aplnra* in LR patterning. Compared with control morphants, the hearts were smaller (Fig. S2 D-E and Fig. 1. B-D) and defective in looping in *aplnra* morphants (Fig. 1 B-D, O), but no distinct neural epithelium laterality was observed (Fig. 1 Q). At 72 hours post fertilization (hpf), the embryos displayed abnormal morphology, and the liver laterality was also disturbed in *aplnra* morphants (Fig. 1 F-G, P), displaying right-sided (Fig. 1 G, P) and both-sided liver (Fig. 1 F, P). Since *aplnra* and *aplnrb* are involved in regulating heart progenitor development in a redundant way [13, 16], we explored whether *aplnrb* also contributed to organ LR patterning. The experiments indicated that although *aplnrb*MO injection (500  $\mu$ M) resulted in the heart disappearing, deformed embryos ([13, 18] and Fig. S2 C) and head asymmetry (Fig. 1 M, Q), which prevented an analysis of heart laterality, titrating the concentration of *aplnrb*MO to 100  $\mu$ M gave rise to 18.2% and 17.5% of embryos displaying heart and

liver laterality defects, respectively (Fig. 1 O, P), without clearly deformed embryos (Fig. S2B). Furthermore, coinjecting *aplnra*MO (400 μM) and *aplnrb*MO (100 μM) resulted in 40.2% of embryos displaying a liver laterality defect (Fig. 1 H-J, P). This ratio was higher than that in *aplnra* morphants (Fig. 1 P, 27.3%). These data indicated the redundancy of *aplnra/b* in organ LR patterning. To confirm the specific role of *aplnra* in organ LR patterning, we tried to rescue the organ LR patterning defect by coinjecting *aplnra* MO and *aplnra* mRNA together into the embryos. After titrating the concentration of *aplnra* mRNA, we found that *aplnra* mRNA injection (20 ng/μl) partially restored the LR defect in *aplnra* morphants (Fig. 1 O, P).

The CRISPR/Cas9 system has been broadly used

in gene editing in zebrafish [34-36]. The high editing efficiency gave us the chance to analyze the role of the *aplnra* gene in Founder(Go) zebrafish embryos [35, 37]. To further confirm the specific role of *aplnra* in LR patterning, we designed and synthesized 4 guide RNAs for *aplnra* *in vitro* and then coinjected them with Cas9 protein into the cytoplasm at the one-cell stage to edit the genome of *aplnra* gene. The results demonstrated that, when the *aplnra* gene was edited (Fig. S3), the heart and liver LR defect phenotype in these embryos was also observed (Fig. 1 P and Fig. S3), which further confirmed the role of *aplnra* in organ LR asymmetry patterning.

All the data above suggest the specific role of *aplnra* in LR patterning, *aplnra* and *aplnrb* regulate organ LR asymmetry patterning in a redundant way.

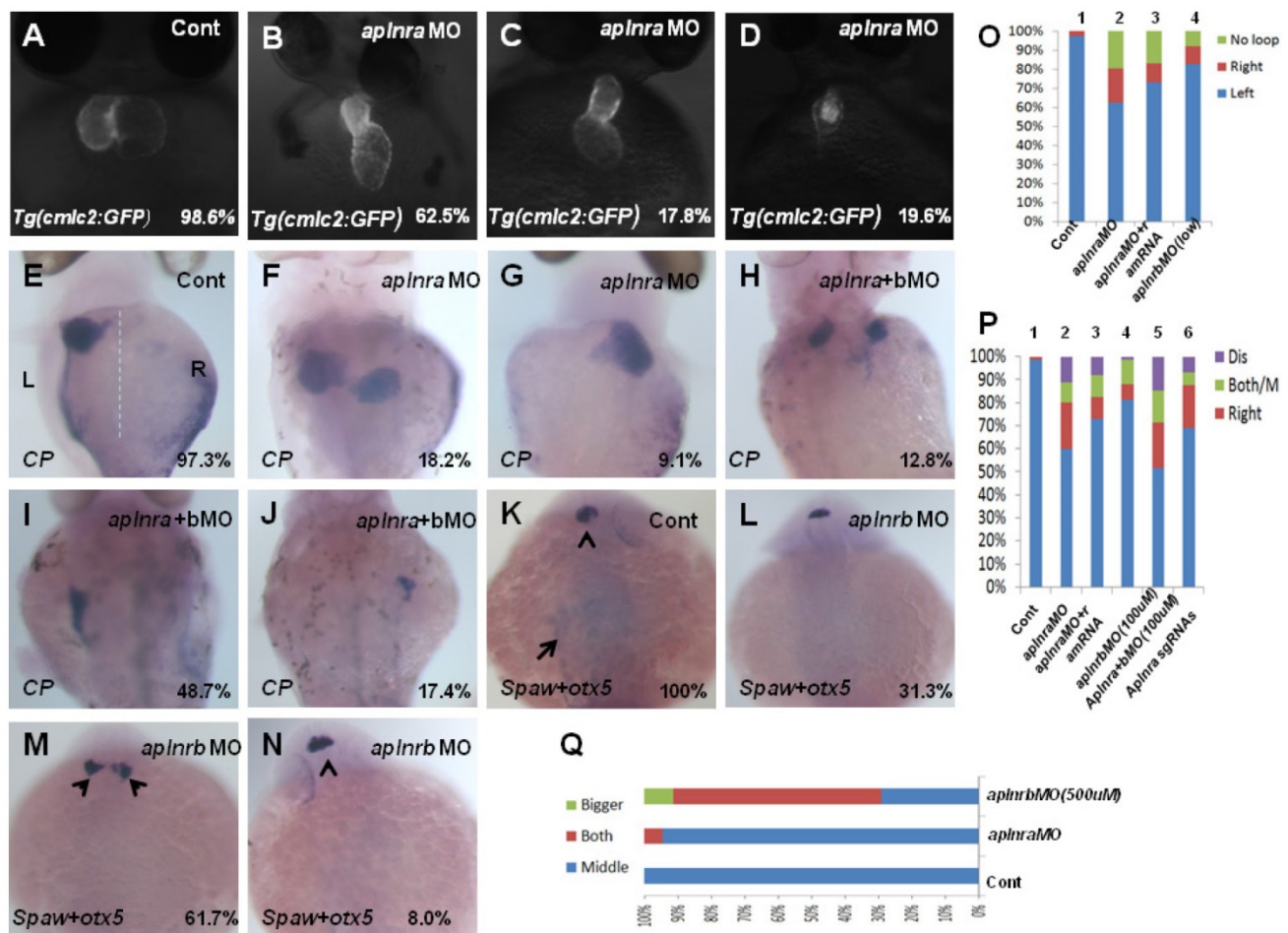


**Figure 1. Organ left-right lateral defect in embryos treated with different ways.** (A-D, O) The pattern of heart displayed in controls and *aplnra/b* morphants. Compared with controls (A, 98.6%, n=72), embryos injected with *aplnra* MO displayed normal-loop (B, 62.5%, n=112; p<0.01), reversed-loop (C, 17.8%, n=112; p<0.01) and no loop (D, 19.6%, n=112; p<0.01). (O, column 1 to 4) The cartogram of heart LR defect for embryos treated with different MOs or mRNA. Only more than 18.2% of *aplnrb* morphants displayed heart LR defect (O, column 4, n=115; p<0.05). *aplnra* mRNA injection (O, column 3, 26.8%, n=71; p<0.05) partially rescued the heart LR defect in *aplnra* morphants (O, column 2, 37.5%, n=112). (E-J, P). While 97.3% of control embryos showed left-sided expression of *cp* (E, n=112), 18.2.0% (F, n=176, p<0.01), 9.1% (G, n=176, p<0.05) and 10.8% (P, n=176, p<0.05) of *aplnra* morphants showed both sided and right-sided expression of *cp*, or disappear. (H-J, P). Compared with that in *aplnra* morphants, *aplnra* mRNA partially rescued liver LR defect (24%, n=121, p<0.05). In *aplnra/b* double morphants, the expression of *cp* was greatly downregulated (100%, n=195, p<0.001), and more embryos displayed liver LR defect (H-J, P, 51.3%, n=195, p<0.05) than that in *aplnra* morphants (P, 38.1%, n=176). In embryos injected with *aplnra* sgRNAs and Cas9 protein, 15.8%; and 6.4% of them displayed right sided and both sided/middle liver (P, n=233, p<0.05). (K-N, Q). *otx5* was expressed in the middle telencephalon. All the embryos injected with Cont MO displayed the expression of *otx5* in the middle telencephalon (K, 100%, n=32, and Q, column 1). While 61.7% of embryos injected with *aplnrb* MO showed both-sided *otx5* in telencephalon (M, Q, n=34), only 5.5% of *aplnra* morphants displayed both-sided *otx5* (Q, 37). For observation, heart, ventral view; *cp*, *spaw* and *otx5*, dorsal view.

### Asymmetric *Nodal/spaw* in the LPM is disturbed when *aplnra/b* is downregulated

The crucial role of *Nodal/spaw* in LR patterning was shown in previous studies [21-23]. Downregulation of *Nodal/spaw* leads to organ laterality defect [38]. To reveal how *aplnra/b* regulates organ laterality, first we examined the left-sided *Nodal/spaw* in embryos injected with *aplnra*MO. The left-sided *Nodal/spaw* was disturbed in *aplnra* morphants, displaying both-sided, right-sided and disappeared *spaw* expression patterns (Fig. 2 A). Since *aplnra* and *aplnrb* regulate liver laterality in a redundant way (Fig. 1 P), we continued to evaluate whether left-sided *Nodal/spaw* was affected in embryos injected with *aplnrb*MO or *aplnra*MO+*aplnrb*MO. In most embryos injected with *aplnrb*MO or *aplnra*+*b*MO, the left-sided *Nodal/spaw* disappeared (Fig. 2 B, and Fig. S4). Furthermore, we sequentially checked *lefty2*, the downstream gene of *spaw* in *aplnra* morphants, and found that the left-sided *lefty2* expression pattern in the heart field was substantially downregulated (Fig. 2 C, D), which was consistent

with that of *spaw* in *aplnra* morphants. The substantial downregulation of *lefty2* in the heart field coincided with the role of *aplnra* in heart progenitor development, i.e., *aplnra* loss of function substantially downregulates heart progenitor development [12, 16]. The data above suggest that the left-sided *Nodal/spaw* or *lefty2* were not only disturbed but also downregulated in *aplnra* morphants (Fig. 2; Fig. S4). To determine when the downregulation of *Nodal* signaling was initiated, we examined the expression of *lefty1* and other *Nodal*-related genes at the gastrulation stage. The experiments indicated that the *Nodal*-related gene *sox32*, *ndr2* and *mxtx2* were downregulated at 70% epiboly (Fig. S4). These data demonstrate that, from the late gastrulation stage, *Nodal*-related genes started to be downregulated. At the somite stage, in addition to the downregulation of *Nodal* signaling, the left-sided *Nodal/spaw* and the downstream gene *lefty2* were also randomized. These data suggest *aplnra/b* signaling contributes to organ LR patterning via the *Nodal/spaw* signaling pathway.

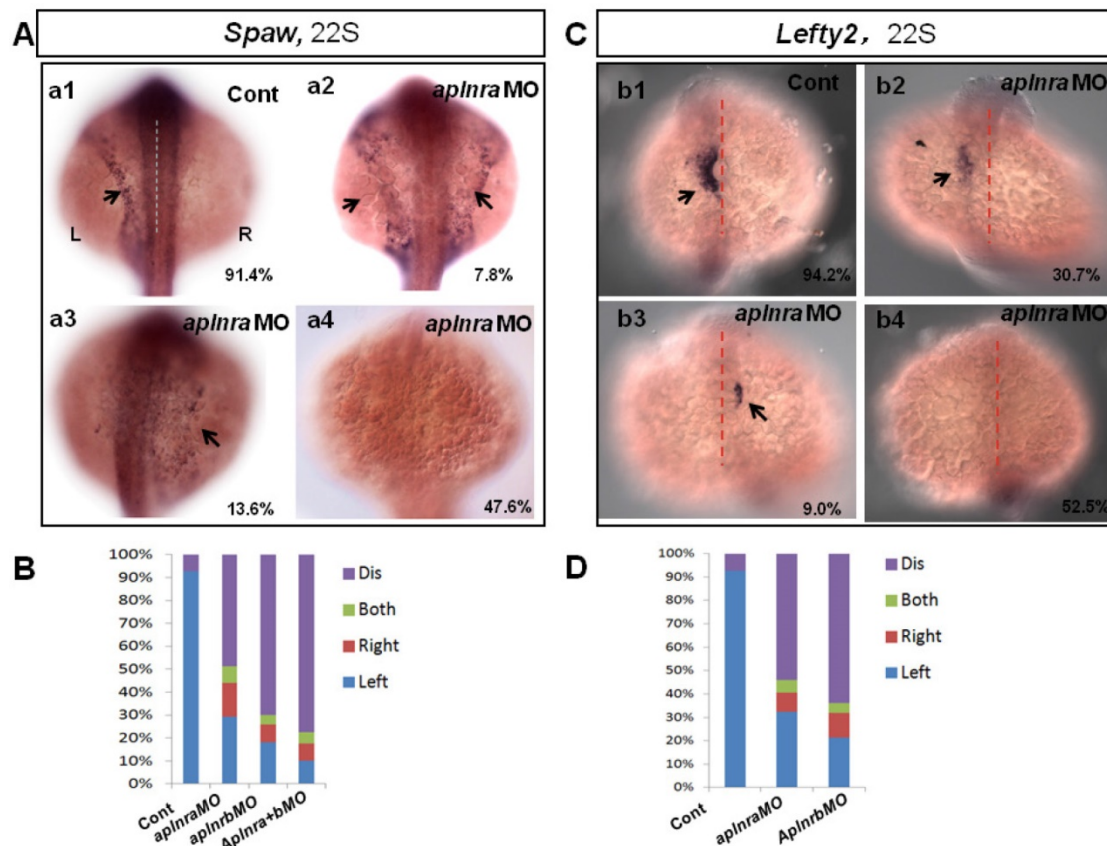


**Figure 2. Expression of left-sided *Nodal* signaling in LPM.** (A. a1-a4, B) Expression of left-sided *spaw* in embryos. In control embryos, near all the embryos expressed left-sided *spaw* (A. a1, 91.4%, n=93). While in *aplnra* and *aplnrb* morphants, left-sided *spaw* expression pattern was changed (A. a2-a4, B), 13.6% ( $p>0.05$ ), 7.8% and 47.6% ( $p<0.001$ ) of *aplnra* morphants expressed right-sided, both-sided *spaw* or *spaw* disappeared (B, middle-left column, n=103). 10.2% ( $p<0.05$ ) and 6.1% ( $p>0.05$ ) of *aplnrb* morphants showed right-sided and both sided *spaw* (B, middle-right column, n=98), majority of *aplnrb* morphants showed no staining for *spaw* (B, middle-right column, n=98,  $p<0.001$ ). (C. c1-c4, D) The expression of left-sided *lefty2* in the heart progenitor field. In the control embryos, *lefty2* was expressed in the left side of heart progenitor field (C.c1, 94.2%, n=52). *lefty2* was down-regulated in *aplnra* morphants (C. c2-c4), the left-sided expression pattern was also perturbed (C. c2-c4, D), with 9.0%, 6.3% and 52.5% of embryos showing right-sided, both-sided *lefty2* and *lefty2* disappeared, respectively (C. c2-c4; D, middle column, n=74). The *lefty2* expression pattern in *aplnrb* morphants (D, right column, n=93) was similar to that in *aplnra* morphants (D, middle column, n=74), but more embryos had no staining for *lefty2* in *aplnrb* morphants (D, right column, n=93) than in *aplnra* morphants (D, middle column, n=74). All the embryos were observed from dorsal view. L, Left; R, Right.

### *Aplnra* but not *aplnrb* dominantly regulates KV formation and ciliogenesis

Previous studies and our current research indicated that *aplnra* but not *aplnrb* is expressed in the DFCs at the gastrulation stage ([11, 18] and Fig. S1). In zebrafish, DFCs will form the KV at the early somite stage, and defective KV morphogenesis or defective ciliogenesis (or functional defect) will give rise to disturbed left-sided *Nodal/spaw* and subsequent organ LR defect [24, 26, 27]. To determine whether *aplnra/b* regulated KV morphogenesis or ciliogenesis, we analyzed the KV/cilia development in *aplnra* or *aplnrb* morphants. Compared with control morphants, at the 10-12 somite stage, the KV was smaller in a majority of *aplnra* morphants (Fig. 3 A-D) while not in *aplnrb* morphants (Fig. 3 D). Further, we examined the cilia development and found that *aplnra* morphants displayed a slightly shorter cilia than control morphants (Fig. 3 F, I). The cilia numbers were also decreased in *aplnra* morphants (Fig. 3 F, H). In *aplnrb*

morphants, no distinct difference in cilia length or cilia number was observed when compared with control morphants (Fig. 3 G, H, I). To assess the specific role of *aplnra* in KV formation and ciliogenesis, the *aplnra* mRNA was used to rescue the KV morphogenesis and ciliogenesis defects in *aplnra* morphants. The results showed that the KV morphogenesis and ciliogenesis defects in *aplnra* morphants were partially rescued by coinjecting with *aplnra* mRNA (Fig. 3 D, H, I). Since *aplnra* expression was also found in DFCs, we studied whether *aplnra* loss of function in DFCs would lead to KV morphogenesis defect. Indeed, injecting *aplnra* MO at 256-512 cell to specifically downregulate the function of *aplnra* resulted in a KV morphogenesis defect (Fig. S5). In addition, DFC-specific downregulation of *aplnra* resulted in randomized *spaw* and the sequential organ LR defect (Fig. S5). These data show that *aplnra* but not *aplnrb* dominantly regulates KV formation and ciliogenesis during the early somite stage.

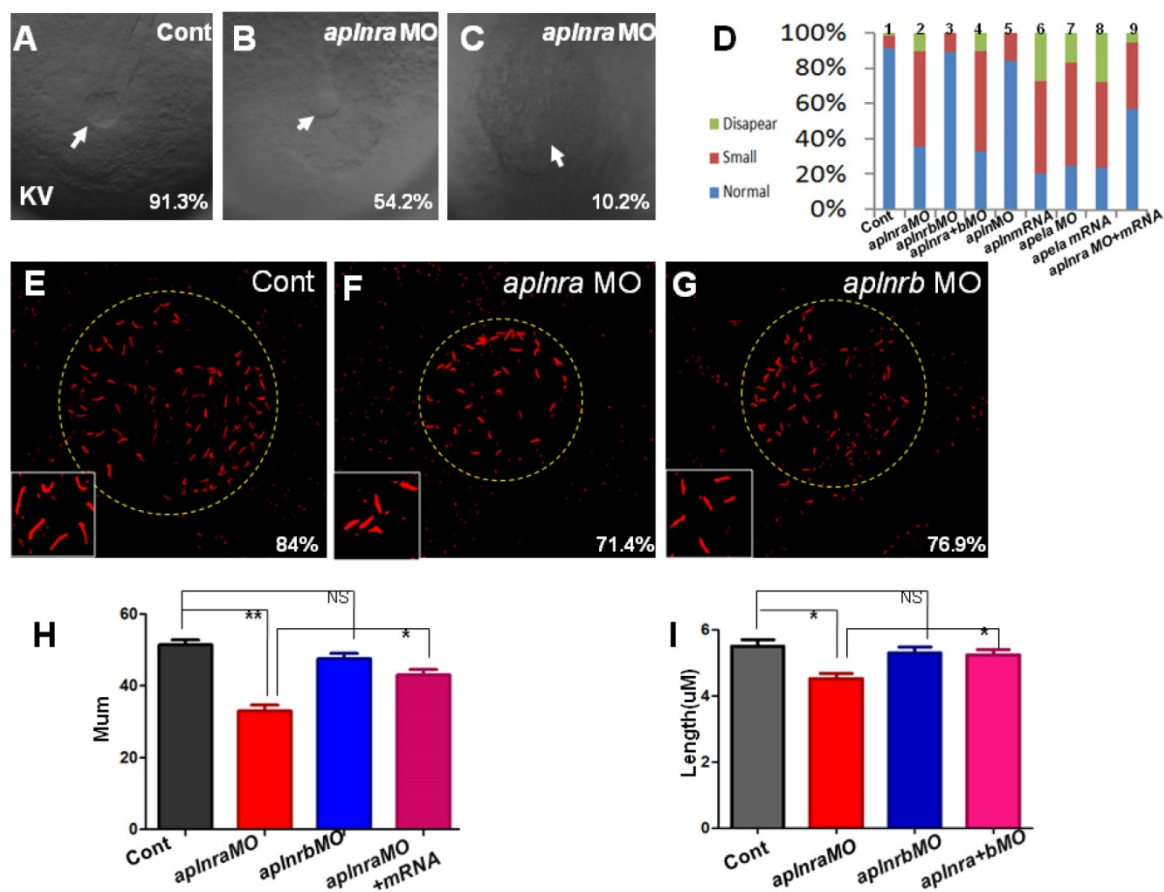


**Figure 3. KV morphogenesis and Ciliogenesis in treated embryos.** (A-D) In control, 91.3% of embryos showed normal KV (A, n=181), but 35.6% ( $p<0.001$ ), 54.2% ( $p<0.001$ ) and 10.2% ( $p<0.001$ ) of embryos injected with *aplnra* MO showed normal KV, smaller KV and no KV, respectively (B, C and D. column 2, n=175), this kind of KV phenotype also can be found in *aplnra*+*b* morphants (D. column 4, n=213,  $p<0.001$ ) or *apela* morphants (D. column 7, n=208,  $p<0.001$ ), embryos injected with *apela* mRNA (D. column 8, n=153,  $p<0.001$ ) or embryos injected with *apln* mRNA (D. column 6, n=135,  $p<0.001$ ). In *aplnrb* or *apln* morphants, no distinct phenotype about KV was discovered (D. column 3(n=147) and column 5, n=193). Injection of *aplnra* mRNA partially restored the KV phenotype in *aplnra* morphants (D. column 9, n=116,  $p<0.05$ ). (E-I) In the KV, compared with that in control morphants (E and H, n=25), the cilia number is decreased in *aplnra* morphants (F and H, n=28,  $p<0.01$ ), difference was also found about the length of cilia (F, I, n=12,  $p<0.05$ ). In *aplnrb* morphants, only mild difference about cilia number and cilia length was observed (G, H, I, n=9,  $p>0.05$ ). Co-injection of *aplnra* mRNA with *aplnra* MO in the embryos resulted that the number (G, H, n=26,  $p<0.05$ ) or length of cilia (G, I, n=14,  $p<0.05$ ) was closed to that in control. \*,  $p<0.05$ ; \*\*,  $p<0.01$ ; NS, not significant.

### **Foxj1a is downregulated in *aplnra* morphants**

In zebrafish and mouse, the Node/KV plays an important role in initiating asymmetric *Nodal/spaw* in LPM [3, 29, 39-41]. At the gastrulation stage, the DFCs move together to the tailbud and then form the KV at the early somite stage [42, 43]. During this process, decreasing the DFC number or disturbing the critical signaling pathways, such as FGF or Wnt signaling, leads to deformed KV morphogenesis or a ciliogenesis defect [28, 44]. To determine how KV morphogenesis and ciliogenesis were disturbed in *aplnra* morphants, we checked whether the primordial cells of KV in *aplnra* morphants were intact at the late gastrulation stage. In zebrafish, *sox17* is generally used as the marker of DFCs. First we examined the expression of *sox17* under *aplnra* loss of function. *sox17* showed three kinds of expression pattern in *aplnra* morphants, 1) similar to that of control (Fig. 4 B), 2) scattered expression (Fig. 4 C) and 3) decreased expression (Fig. 4 D). By measuring the area of *sox17* expression, we confirmed that the area of *sox17* expression was slightly smaller than that in controls (Fig. 4 E e2, red group). However, the downregulation of *sox17* in DFCs was not found in *aplnrb* morphants (Fig. 4 E e3, pink group).

*Fgf8*, *dnah9* and *foxj1a* are involved in KV formation and ciliogenesis [20, 28, 33, 39, 45]. *dnah9* also lies downstream of FGFR signaling to regulate ciliogenesis [39]. To study how *aplnra* regulates the development of KV and cilia, we examined the expression of *fgf8* and its downstream genes *erm*, *dnah9* and *foxj1a*. At the 2-somite stage, *in situ* and Q-PCR experiments showed that there was no distinct difference in *fgf8* (Fig. S6 A, C) or *dnah9* expression (Fig. S6 D, E) between *aplnra* morphants and control embryos. Interestingly *erm*, the downstream gene of *fgf8*, was upregulated in *aplnra* morphants (Fig. S6 B, C). Finally, we found that *foxj1a* was greatly downregulated (Fig. 4 F-H), which was also confirmed by analyzing the area of *foxj1a* expression (Fig. 4 I) and Q-PCR (Fig. 4 J). To examine whether *foxj1a* mediates the role of *aplnra* in KV/cilia development, we performed rescue experiments. The results indicated that transient expression of *foxj1a* by injecting *foxj1a* mRNA partially rescued the KV phenotype and the heart LR patterning defect in *aplnra* morphants. In *aplnra* morphants, 54.2% of embryos displayed smaller KV (Fig. S 7 B), while 78.6% of embryos coinjected with *aplnra*MO and *foxj1a* mRNA displayed slightly larger KV than that in embryos injected with *aplnra*MO (Fig. S7 C). For heart LR patterning, only 22.1% of embryos coinjected with *aplnra*MO and *foxj1a* mRNA displayed the LR patterning defect (Fig. S 7 E, F). This ratio was lower than that in *aplnra* morphants (Fig. 1 O, column 2,

37.5%). All these data demonstrate that *foxj1a* but not *fgf8* was downregulated in *aplnra* morphants and that *foxj1a* possibly at least partially mediated the role of *aplnra* to regulate KV morphogenesis and the subsequent organ LR patterning.

Our early data in this study showed that injection of *aplnrb*MO enhanced the organ LR patterning defect in *aplnra* morphants (Fig. 1 P, column 5). Although *aplnrb* loss of function did not lead to distinct defective KV and ciliogenesis (Fig. 3), we could not exclude the possibility that *aplnrb* was partially involved in helping *aplnra* to regulate the expression of cilia-related genes. Here, we examined this possibility, and the result indicated that no distinct difference in the expression of cilia-related genes was observed between *aplnrb* morphants and control morphants (Fig. 4 E, I; Fig. S6). We also did not find a significant difference in the expression of cilia-related genes between *aplnra* morphants and *aplnra+b* morphants (Fig. 4 E, I and Fig. S6). This result further confirmed that *aplnrb* contributes to organ LR patterning in a KV/cilia-independent way.

### **Apela and *apln* regulate organ LR asymmetry**

The first identified endogenous ligand of *aplnra/b* was *apelin(apln)* [18], the late ligand. More recently, *apela* was identified to work as the early endogenous ligand of *aplnra/b* in heart development [12]. To evaluate whether *apela/apln* work as the ligands of *aplnra/b* during LR patterning, we examined the expression patterns of *apela/apln* from gastrulation to somitogenesis. The results demonstrated that, starting from the bud stage, *apln* was expressed in the midline (Fig. S8 Aa3-a8) and heart progenitors (Fig. S8 Aa7, left arrow; a8, down arrow), while it was not expressed in the KV epithelium (Fig. S8 Aa6, the down black arrow). *Apela* was expressed ubiquitously at 75% epiboly (Fig. S8 Bb1), in the midline and presomite mesoderm (PSM) at the bud stage (Fig. S8 Bb2-3), in the midline and KV epithelium at the 4-somite stage (Fig. S8 B4-b5, white arrow), and in the midline and heart progenitors at the 15-somite stage (Fig. S8 Bb6-b8, arrow). These expression data demonstrate that the expression patterns of *apln/apela* are different at early developmental stages. If *apln/apela* work as the ligands of *aplnra/b* during LR patterning, they might play different roles during this process. To evaluate this hypothesis, we continued to analyze the organ laterality in *apela* morphants and *apln* morphants. In *apela* morphants, the majority of embryos had no heart or a very small heart (Fig. S9), consistent with a previous report [12]. This phenotype blocked the analysis of heart LR in *apela* morphants. At day 3, *in situ* staining for *cp* demonstrated that liver laterality was perturbed in *apela* morphants (Fig. 5

Aa2-a3), similar to the phenotype in *aplnra* morphants (Fig. 1 G,P). In addition, the liver LR patterning defect was also observed in *Tg(fabp10:GFP)* transgenic embryos injected with *apela* MO (Fig. 5 Bb2-b3). To confirm the general role of *apela* in LR patterning, *otx5* was used to examine the head laterality(46, 47). We found *otx5* was expressed in both sides of the head in major of *apela* morphants (Fig. 5 C), phenocopying *aplnrb* morphants (Fig. 1 M, Q). In *apln* morphants, the heart progenitors were not decreased, but the heart (Fig. 5 D, H and Fig. S10 A) and liver (Fig. 5 E,G and Fig. S10 B) LR patterning were disturbed. To further confirm the specific roles of *apela/apln* in organ LR patterning, we also used the CRISPR/Cas9 method to edit the *apln/apela* genes and evaluated the roles of *apela/apln* in LR patterning. The results indicated that, when *apela* or *apln* genomic DNA was edited (Fig. S11), the liver LR defect was also observed (Fig. 5 G, columns 8 and 9 and Fig. S11). These data suggest that, as the endogenous ligands, *apela/apln* were involved in regulating organ LR patterning. In a

previous report, as the ligand of *aplnra/b*, *apela* or *apln* gain of function led to decreased heart progenitor cell number [18], Here, *apela* or *apln* gain of function also resulted in a liver LR patterning defect (Fig. 5 F, G; and Fig. S10), implying *apela/apln* and the receptors *aplnra/b* are in the same cascade in LR patterning.

Given that *apela/apln* and *aplnra/b* work in the same cascade in LR patterning, simultaneously downregulating *aplnra/b* and their ligands *apela/apln* will result in a stronger LR defect phenotype than that in *aplnra* morphants or *apela/apln* morphants. Indeed, the liver LR asymmetry defect in *apela* morphants was enhanced by coinjecting with *aplnra* MO or *aplnrb* MO (Fig. 5 G column 6 and column 7), further confirming that *apela/apln* and the receptors *aplnra/b* were in the same cascade in LR patterning. Since *apela* was expressed from the early stage and *apln* was expressed in the midline from the late gastrulation stage [12, 18, 21] (and Fig. S8 Aa3-a8), it seems that the ligands *apela* and *apln* sequentially couple with *aplnra/b* to regulate LR patterning at different stages.

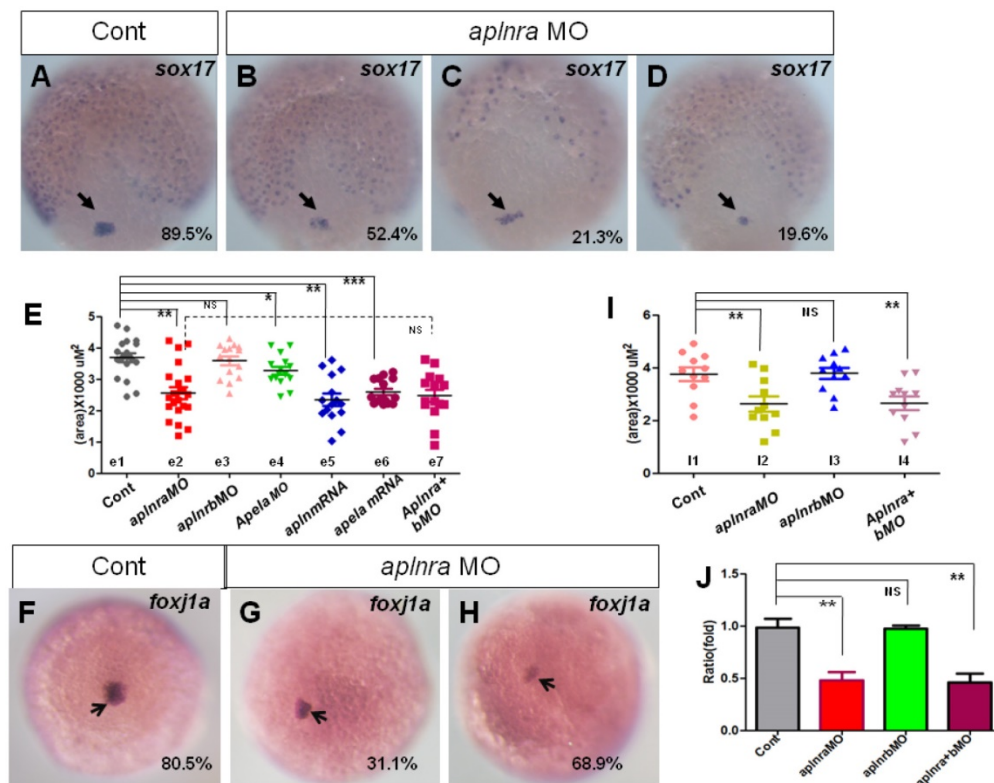


**Figure 4. Expression of *sox17* and *foxj1a*.** (A-E) Expression of *sox17* in DFCs at 90% epiboly. In control embryos, 89.5% of embryos showed normal expression (A, n=88). In *aplnra* morphants, three kinds of expression pattern were discovered: mild decreased (B, 52.4%, n=89, p<0.001), scattered (C, 21.3%, n=89, p<0.001) and decreased (D, 19.6%, n=89, p<0.01). The area of *sox17* expression was measured and in control embryos, the average level was  $3.68 \times 10^3 \text{ uM}^2$  (E. e1 group, n=19), the average area in *aplnra* morphants was  $2.55 \times 10^3 \text{ uM}^2$  (E. e2 group, n=22, p<0.05). *Sox17* expression areas were also measured for *aplnrb* morphants, *aplnra+b* morphants, *apela* morphants, embryos injected with *apln* mRNA and embryos injected with *apln* mRNA, respectively (E, e3-e7 group). The average areas were  $3.63 \times 10^3 \text{ uM}^2$  (E, e3 group, *aplnrb* morphants, n=15, p>0.05),  $2.53 \times 10^3 \text{ uM}^2$  (E. e7 group, *aplnra+b* morphants, n=15),  $3.28 \times 10^3 \text{ uM}^2$  (E, e4 group, *apela* morphants, n=15, p<0.05),  $2.46 \times 10^3 \text{ uM}^2$  (E, e5 group, *apln* mRNA, n=15, p<0.01) and  $2.64 \times 10^3 \text{ uM}^2$  (E, e6 group, *apela* mRNA, n=15, p<0.001), these data indicated *sox17* expression was down regulated in all these treated embryos, excepted for *aplnrb* morphants. (F-J) Analysis of *foxj1a* expression. *Foxj1a* was expressed in DFCs at 90% epiboly in control (F) and treated embryos (G, H). Compared with control embryos (F, 80.5%, n=82), *foxj1a* was greatly down regulated in *aplnra* morphants (H-I, 68.9%, n=87, p<0.001) as well in *aplnra+b* morphants (I, 65.7%, n=76, p<0.001), but not in *aplnrb* morphants (I, 18.9%, n=74, p>0.05). *Foxj1a* expression area in control embryos, *aplnra* morphants, *aplnrb* morphants and *aplnra+b* morphants were average  $3.75 \times 10^3 \text{ uM}^2$ ,  $2.56 \times 10^3 \text{ uM}^2$ ,  $3.57 \times 10^3 \text{ uM}^2$  and  $2.39 \times 10^3 \text{ uM}^2$  respectively (I). Compared with that in control embryos, q-PCR experiment showed the quantity of *foxj1a* expression in *aplnra* morphants and *aplnra+b* morphants were down-regulated with 0.48 folds and 0.46 folds respectively, while the expression of *foxj1a* in *aplnrb* morphants was not affected (J). \*, p<0.05; \*\*, p<0.01; \*\*\*, p<0.001; NS, not significant.

### Apela loss of function depresses left-sided Nodal/spaw in the LPM in a KV-dependent way

Our current data showed that *apela/apln* worked as the ligands of *aplnra/b* to regulate organ LR patterning, but how they regulated LR patterning was unknown. The different expression patterns between *apela* and *apln* gave rise to the possibility that the mechanisms by which *apela/apln* regulate LR patterning are different. To evaluate this possibility, we examined the KV development and the expression pattern of *Nodal/spaw*. In *apela* morphants, the KV morphogenesis was affected, most of embryos displayed smaller KV (Fig. 6 Aa1-a3, B), similar to the phenotype in *aplnra* morphants (Fig. 3 B-D). In contrast, the defective KV formation was not found in *apln* morphants (Fig. 6 B). This result implied the possibility that *apela* but not *apln* works as the ligand of *aplnra* to regulate KV development and the downstream left-sided *spaw* in the LPM. Indeed, further experiments showed that left-sided *spaw* (Fig.

6 C.c2-c5, D) and *lft2* (Fig. 6 E.e2-e4, F) were substantially downregulated, and the left-sided expression pattern of both of them was disturbed in *apela* morphants (Fig. 6 C,E), similar to that in *aplnra* morphants (Fig. 2). In *apln* morphants, although the left-sided expression patterns of *spaw* and *lft2* were also disturbed (Fig. 6 D, F), neither of them was substantially downregulated.

Since *apela* was found to be expressed in KV epithelium, we analyzed whether *apela* loss of function in DFCs resulted in LR patterning defects. As shown in Fig. S5, the KV development and left-sided *spaw* expression were all disturbed, but *spaw* was not downregulated in embryos with *apela* loss of function in DFCs (Fig. S5 Aa4 and Dd4). Heart and liver LR patterning defect were also observed in these embryos (Fig. S5 Bb4 and Cc4). These data further demonstrate that *apela* is involved in LR patterning via a KV/cilia-dependent cascade.

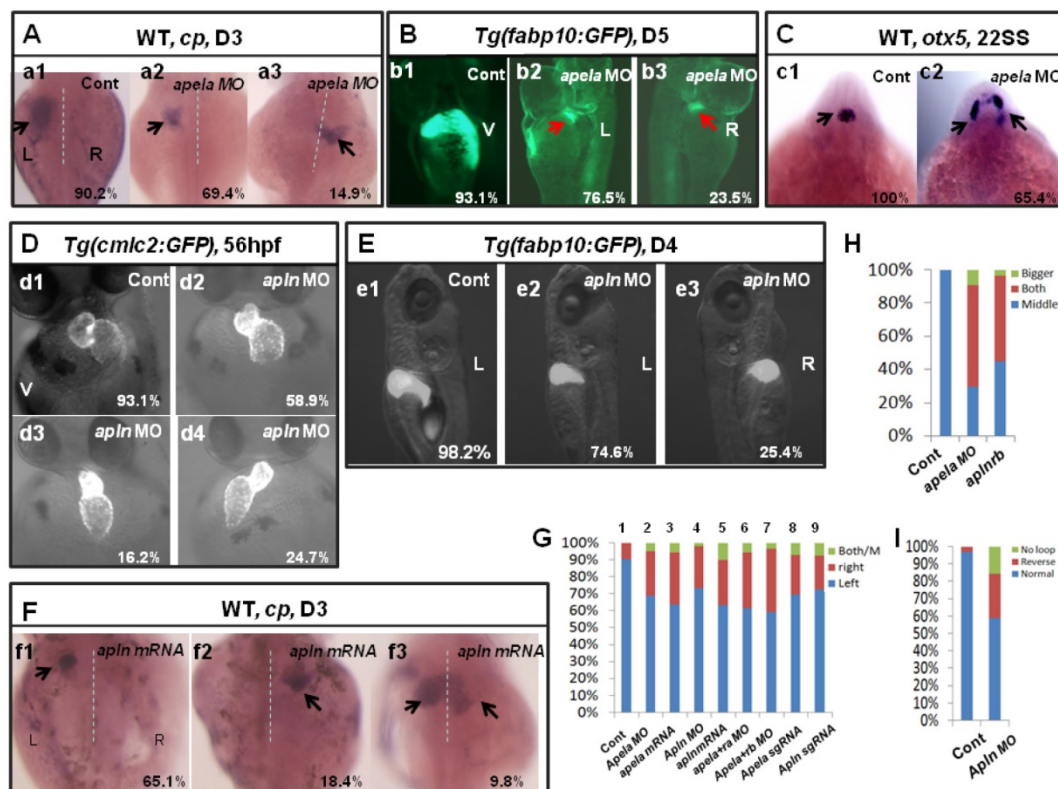


**Figure 5. Organ LR asymmetry defect in embryos with *apln* ligands loss or gain of function.** (A, G) Majority of control embryos expressed left-sided liver marker *cp* in day 3 (A. a1, G. column 1, 90.2%, n=51). Liver LR asymmetry was disturbed in *apela* MO injected embryos (A. a2-a3, G. column 2, 30.6%, n=121, p<0.01) and *apela* mRNA injected embryos (G. column 3, 34.9%, n=103, p<0.01). In transgenic line *Tg(fabp10:GFP)*, the liver LR defect was also observed, displayed left-sided and right-sided liver in 76.5% and 23.5% of *apela* morphants, respectively (B. b2 and b3, n=51), but the GFP in liver region started to express in day 5 (B. b2 and b3). (C) Head marker *otx5* was expressed in the middle telencephalon (C. c1, H. column 1, 100%, n=32), but many of *apela* morphants (C. c2, H. column 2, 65.4%, n=26) and *aplnrb* morphants (H. column 3 61.7%, n=34) showed both-sided *otx5* in telencephalon. (D, I) *Apln* loss of function resulted heart LR asymmetry defect (D. d2-d4, I). displayed reversed loop (D. d4, I, 24.7%, n=117, p<0.05), normal loop (D. d2, I, 58.9%, n=117, p<0.01) and linear heart (D. d3, I, 16.2%, n=117, p<0.05). (E. e1-e3, G) In *apln* morphants, liver development was not delayed (E), but 25.4% liver LR asymmetry defect was found (E. e2-e3, G. column 4, n=185, p<0.001). *Apela* mRNA or *apln* mRNA gain of function also resulted in liver LR asymmetry defect, 34.9% (p<0.01) and 37.2% (p<0.01) of embryos displayed right-sided or both-sided expression of *cp* (G. column 5, n=97). When compared with the liver LR defect in *apela* morphants (G. column 2, 30.6%, n=121), high ratio of embryos co-injected with *apela* MO and *aplnra* MO (G. column 6, 37.1%, n=70), or embryos co-injected with *apela* MO and *aplnrb* MO (G. column 7, 40.0%, n=91) showed liver LR asymmetry defect. In embryos injected with *apela/apln* sgRNAs with Cas9 protein, the livers also showed left right asymmetry defect (G. column 8 and 9). L, left; R, right; V, ventral view; D3, day 3; D5, day 5.

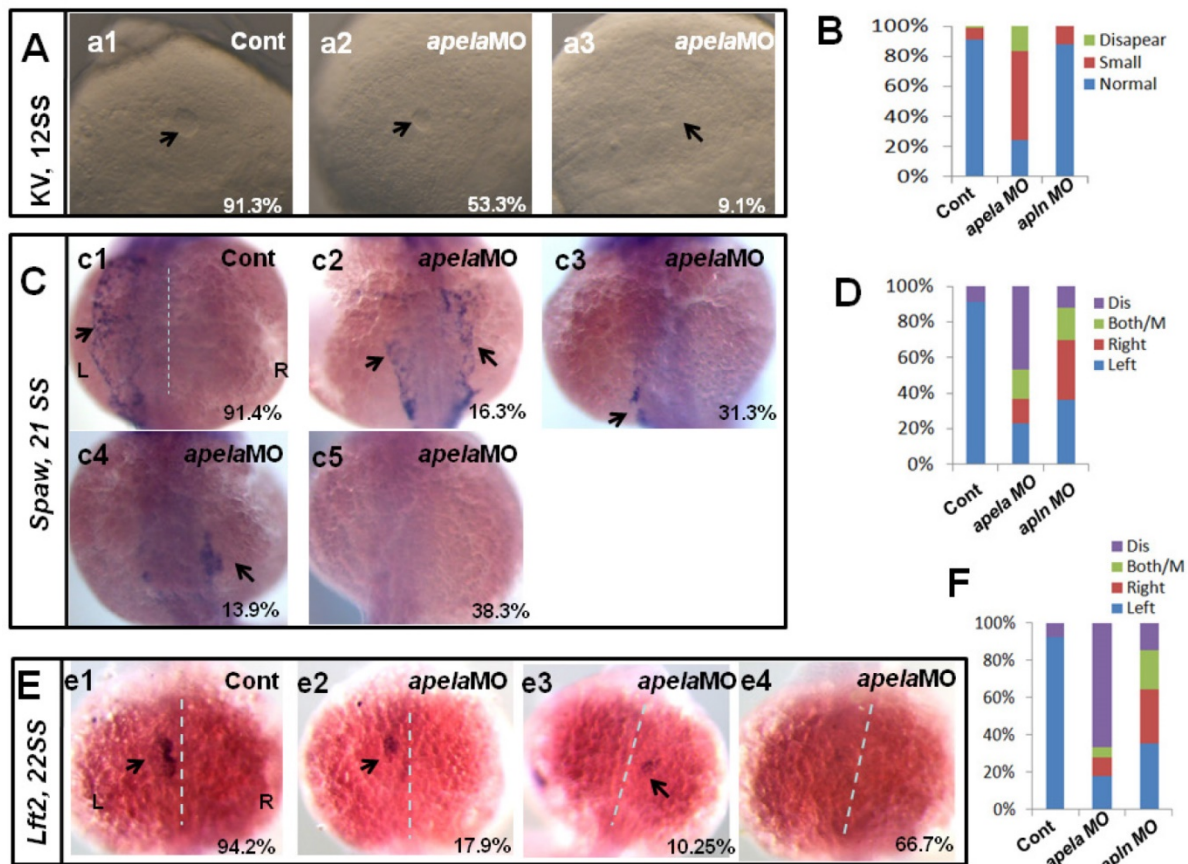


**Figure 6. KV morphogenesis and left-sided Nodal signaling in *apela* morphants.** (A-B) In control, 91.2% of embryos showed normal KV (A, n=136), but 37.6%, 53.3% and 9.1% of embryos injected with *apela* MO showed normal KV, mild smaller KV and no KV, respectively (B, C and D, column2, n=178). (C, c1-c5, D) Majority of control morphants expressed left-sided *spaw* in the LPM (C, c1, D left column, 91.4%, n=35). In *apela* MO morphants, 31.3%, 13.9% and 16.3% of embryos showed left-sided *spaw*, right-sided *spaw* and both-sided *spaw* (C, c2-c4, D middle column, n=30), while the *spaw* expression in most of *apela* morphants couldn't be found (C, c5, D middle column, 38.9%, n=86). (E-F) The Nodal downstream gene *lft2* was checked. Compared with that in control embryos (E, e1, F right column, 94.2%, n=52), *lft2* was down regulated and the left-sided expression pattern was disturbed in *apela* morphants (E, e2-e4, F middle column, n=39), displaying left-sided (17.9%), right-sided (10.25%), both-sided (5.12%) expression and the expression disappeared (66.7%). The disturbed KV morphogenesis and the perturbed *spaw* or *lft2* expression were also observed in *apln* morphants (D, D, F, right column).

Since *aplnra* regulated the expression of *foxj1a* and *erm*, if the ligand *apela* but not *apln* truly couples with *aplnra* to regulate KV formation and ciliogenesis, the expression of *foxj1a* and *erm* in *apela* morphants should be similar to that in *aplnra* morphants. Indeed, the expression of *fgf8* (Fig. 7 A) and *dnah9* (Fig. 7 C) was not affected in *apela* morphants, while *erm* (Fig. 7 B) and *foxj1a* (Fig. 7 D-F) were increased and decreased, respectively, similar to *aplnra* morphants (Fig. 4 G-I). These data suggest that *apela* but not *apln* works as the ligand of *aplnra* to regulate LR patterning in a KV-dependent way.

***Lft1* is downregulated in midline in both *apela* and *apln* morphants**

Our data above showed that *apln* was involved in regulating organ LR patterning and left-sided *spaw* and *lft2*, but this process was independent of KV morphogenesis and *foxj1a* expression. How does *apln* regulate organ LR patterning? Since midline defects lead to randomized expression of *spaw* and *lft2* in a

KV/cilia-independent manner [48], and *apln* is expressed in the midline from the late gastrulation stage to the somite stage [18, 21] (Fig. S8 Aa3-a8), so we hypothesized that *apln* might be involved in regulating midline formation or function. To evaluate this possibility, we examined whether *apln* loss of function affected midline formation. In *apln* morphants, no deformed midline was observed in the living embryos (data not shown), and no decreased expression of *shh* was discovered (Fig. 8 Aa3). We also did not find any distinct difference in the expression of *shh* among the *apela* morphants, *aplnra* morphants, *aplnrb* morphants and *aplnra+b* double morphants (Fig. 8 Aa2-a6, shown by black arrow head). These data show that *apln* (including the early ligand *apela*) and their receptors are not involved in regulating the expression of *shh*, one of the critical genes in the midline to maintain the left-sided *Nodal/spaw* in LPM.

Since intact *lft1* in the midline is vital to ensure left-sided *spaw* expression in the LPM and the later organ LR patterning, we examined whether the

expression of *lft1* was affected in *apl*n morphants. At 20 SS, *lft1* was expressed in 4 domains in wild-type embryos, including the left telencephalon, left heart field, trunk midline and tail midline (Fig. 8 Bb1, shown by the black arrow head). In *apl*n morphants, *lft1* in the trunk midline disappeared or decreased greatly in the majority of embryos (Fig. 8 Bb4-b6, class 3 to class 5; C, the second column). In the control morphants, the expression of *lft1* in the midline was intact (Fig. 8 Bb1, C, column 1). This result indicated that *lft1* in the trunk midline was depressed in *apl*n morphants, implying that *lft1* in the midline mediates the effect of *apl*n to regulate LR patterning.

Since *apela* is expressed in the midline and guides angioblasts to move to the midline [33], and its receptor *apl*nra/b is expressed close to that of *apl*n/*apela*, we supposed that *apela* and the receptors *apl*nra/b were also involved in regulating the expression of *lft1* in the trunk midline. Indeed, further experiments showed that the defective expression pattern of *lft1* was also found in *apela* morphants, *apl*nra morphants and *apl*nrb morphants (C, column 3 to 5). Nearly half of embryos showed greatly decreased *lft1* in the trunk midline in all the morphants. This result provided additional evidence that *apl*n (and *apela*) works as the ligand of *apl*nra/b to regulate organ LR patterning at the somite stage. In summary, at the somite stage, *apl*n/*apela*-*apl*nra/b are involved in the regulation of *lft1* in the trunk midline to maintain the midline function and the subsequent organ LR patterning.

## Discussion

### The complementary role of *apl*nra and *apl*nrb in organ LR patterning

In vertebrates, *apl*n (*apl*nra/b in zebrafish) has multiple roles in organ development and diseases [5, 21, 39, 40, 49]. In mouse, *apl*n regulates cardiac contractility [50], heart looping and vascular maturation [21]. In zebrafish, functions in regulating gastrulation cell movement [14], heart [16-18], angiogenesis [33] and lymphatic system development [19, 20] are also reported. While in regulating heart development, zebrafish *apl*nra and *apl*nrb play different roles via multiple mechanisms: In *apl*nrb mutants, most heart progenitors are absent [18], but in *apl*nra mutants or morphants, the heart progenitors are only decreased [12]. Similarly, the vasculogenesis defect in *apl*nra mutants is not as strong as that in *apl*nrb mutants, but knockdown of *apl*nra enhances the vasculogenesis defect in *apl*nrb mutants [33]. It is possible that the different roles of *apl*nra/b in heart development and angiogenesis come from the different expression patterns of *apl*nra/b. In our

current study, the data demonstrate the critical roles of *apl*nra/b in organ LR patterning (Fig. 1). During this process, *apl*nra and *apl*nrb have redundant roles during liver LR patterning (Fig. 1 H-J, P). Interestingly, the head laterality in *apl*nrb morphants was more severe than that in *apl*nra morphants (Fig. 1 K-Q), phenocopied that in *squint* or MZoop mutants [46]. This result was consistent with a more recent report that Nodal/TGF $\beta$  signaling is greatly downregulated in *apl*nrb mutants [16]. On the role of *apl*nrb in heart LR patterning, although *apl*nrb loss of function results in heart absence or heart size decrease in most of embryos (Fig. S2 Cc2-c4), we still believe the role of *apl*nrb in organ LR patterning is general for all organs, since the left-sided *spaw* was substantially downregulated or disturbed in *apl*nrb morphants (Fig. 2 B, Fig. S4 A, B).

By carefully analyzing the ratio of the heart and liver LR patterning defects in embryos injected with the same MOs, we found that the rates of the heart and liver LR defects were different (Fig. 1 and Fig. 5). Our early studies also found this kind of phenotype [38, 51]. Here, we wanted to know, in the embryos injected with *apl*nra MO, whether the liver LR patterning was also defective in the embryos with a reversed heart loop. We sorted out the *Tg(cmlc2:GFP)* embryos with a reversed heart loop, incubated them to 5 days post fertilization, and then examined the liver LR patterning using *in situ* experiments (Fig. S12). The results demonstrated that, in the embryos with a reversed heart loop, 29.4% of embryos displayed right-sided liver (Fig. S12 Aa1 and a3), while in the embryos with a normal heart loop, 18.7% of embryos displayed right-sided liver (Fig. S12 Bb1 and b3). Clearly, this result indicates that the heart and liver LR defects do not always occur at the same time in the *apl*nra morphants. It also implies that the detailed mechanisms underlying heart and liver LR patterning are at least partially different.

One other interesting phenotype was that *apl*nrb morphants displayed liver and head laterality defects, but no KV morphogenesis defect. For this result, two kinds of data can explain how the organ LR patterning was affected in *apl*nrb morphants. First, although *apl*nrb loss of function did not lead to defective KV development, downregulated Nodal signaling at the gastrulation stage and the somitogenesis stage contributed to the organ LR patterning defect. This explanation is supported by our current data (Fig. 2 B, D and Fig. S4 A,B) and previous reports [16]. Second, at the somite stage, the downregulation of *lft1* in the midline also contributed to the organ LR patterning defect in *apl*nrb morphants (Fig. 8 B, C).

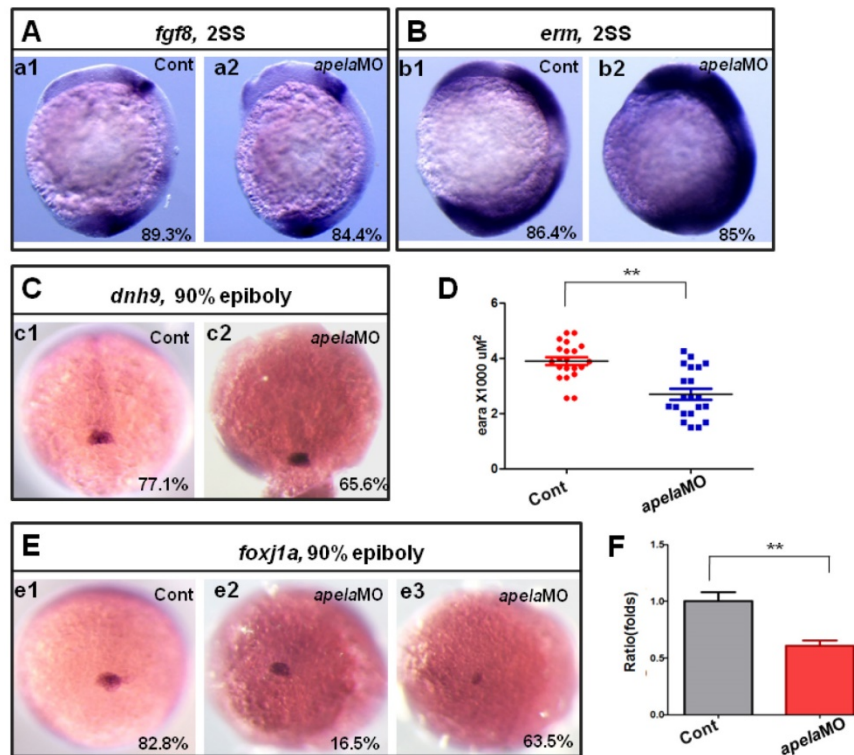


**Figure 7. KV/cilia related signaling pathway analysis in *apela* morphants.** (A-C) Compared with the control embryos (A. a1, B. b1 and C. c1), the expression of *fgf8* and the downstream gene *dnh9* were not changed in *apela* morphants (A. a2, 84.4%, n=32; C. c2, 65.6%, n=32), but the expression of *erm* was up regulated in *apela* morphants (B. b2, 85%, n=20). (E-D) *Foxj1a* was expressed in DFCs. Compared with that in control embryos (E. e1, 82.8%, n=35), *foxj1a* was down regulated in *apela* morphants (E. e3, 63.5%, n=104). The average area of *foxj1a* expression in control embryos and *apela* morphants were  $3.87 \times 10^3 \mu\text{M}^2$  (n=21) and  $2.75 \times 10^3 \mu\text{M}^2$ , respectively (D, n=21,  $p < 0.01$ ). Q-PCR experiment indicated that *foxj1a* expression was down regulated with 0.61 folds compared with that in control embryos (F). \*,  $p < 0.05$ ; \*\*,  $p < 0.01$ .

### ***Aplnra* regulates LR patterning in KV/cilia-dependent and -independent ways**

The mechanism by which organ LR laterality is established is complicated and needs more study [50, 52]. In zebrafish, two events are critical for LR asymmetric signaling initiating and maintenance: normal KV morphogenesis/ciliogenesis and an intact midline [47, 48, 53-56]. Our results first identify the dominant role of *aplnra* in LR patterning (Fig. 1 A-H). In this mechanism, the left-sided *spaw* and *lft2* were perturbed (Fig. 2 A-D), which mediated the disturbed organ LR patterning in *aplnra* morphants. Further data indicated that *foxj1a* in DFCs was downregulated in *aplnra* morphants (Fig. 4 F-J), possibly mediating the role of *aplnra* in regulating KV morphogenesis and ciliogenesis (Fig. 3), the downstream left-sided *spaw*, *lft2* and the subsequent organ LR patterning (Fig. 2 A-D). Since *aplnra* is expressed ubiquitously in the embryos from the dome stage to the late gastrulation stage [12, 14], and in the early somite stage it is also expressed near the midline [33], these data argue against the idea that *aplnra* is involved in regulation of LR patterning in only a KV morphogenesis/ciliogenesis-dependent manner. Indeed, besides the perturbed left-sided *spaw* expression pattern in *aplnra*

morphants (Fig. 2 A), *spaw* was downregulated or disappeared in most *aplnra* morphants (Fig. 2 B) meaning that *aplnra* loss of function not only randomized the left-sided *spaw* in LPM but also depressed the expression of *spaw* in LPM. This result was consistent with the earlier report that Nodal and Nodal-related genes were downregulated in *aplnra* mutants [16] (Fig. S4 C-F). In addition, our previous data showed that *spaw* loss of function resulted in randomized organ LR patterning [38], further supporting the hypothesis that *aplnra* contributes to left-sided *spaw* expression and the sequential organ LR patterning via not only a KV/cilia cascade but also a KV/cilia-independent signaling pathway.

The expression of *aplnra* in the midline at the somite stage encouraged us to investigate the role of *aplnra* in midline development. There was no distinct morphogenesis defect in living *aplnra* morphants, and the expression of *shh* in *aplnra* morphants was intact (Fig. 8 Aa5), while the expression of *lft1* in trunk midline was substantially depressed (Fig. 8 B, C). These data suggest that *aplnra*, besides contributing to KV and cilia development at an early stage, also regulates midline function by regulating the expression of *lft1* at the somite stage. In *aplnra* morphants or mutant embryos, *lft1* was unaffected at the early gastrulation

stage (50% epiboly) [37]. To assess when *lft1* was downregulated in embryos with *aplnra* loss of function, we examined the expression of *lft1* from the shield stage in *aplnra* morphants. The data indicated that *lft1* was slightly downregulated from the shield stage, suggesting downregulation of *lft1* in the midline at the somite stage comes from two separate time points: gastrulation and somitogenesis stage. In brief, *aplnra* contributes to organ LR patterning in KV/cilia-dependent and -independent ways.

**Apela but not *apln* works as the ligand to regulate KV formation and ciliogenesis**

Cardiovascular development defects have been reported in APJ KO mice, but not in Apelin KO mice [3, 21, 41]. Heart contractility defects and disturbed looping were also found in APJ KO mice, but these functional and morphogenic defects do not exist in Apelin KO mice, even though the Apelin KO mice obtained a heart contractility defect during aging and severe heart failure was observed in response to pressure overload [5]. These data from mice suggest the possibility that Aplnr regulates heart development in an apelin-independent manner. This possibility was also confirmed by data from zebrafish. In zebrafish, two endogenous ligands *apela* and *apln*

were discovered [14, 18]. During heart development, *aplnra/b* contribute to heart progenitors specification and migration [13, 16, 18], while only loss of function for the ligand *apela* and not *apln* phenocopies *aplnrb* loss of function [16, 18]. Here, our data further show the specific role of *apela* but not *apln* in KV morphogenesis and ciliogenesis during LR patterning. During the gastrulation and early somite stages, *apela* loss of function resulted in KV development defect and disturbed ciliogenesis (Fig. 3 D, 4 E, 6 A, B), which contributes to, at least partly, the downstream left-sided gene *spaw* expression defect (Fig. 6 C,D) and organ LR defect (Fig. 5 A-C). In this process, it is possible that the downregulated *foxj1a* dominantly contributes to the decreased KV progenitors and the smaller KV in *apela* morphants (Fig. 7 D-F). On the other hand, *apln* was mildly expressed from the late gastrulation stage, and downregulation of *apln* did not lead to abnormal KV morphogenesis (Fig. 3 D), heart or endoderm organ progenitor specification or outgrowth (Fig. 5 D, E and data not shown [18]). Of course, we cannot exclude the possibility that some unknown *aplnr* ligand is also involved in KV morphogenesis.

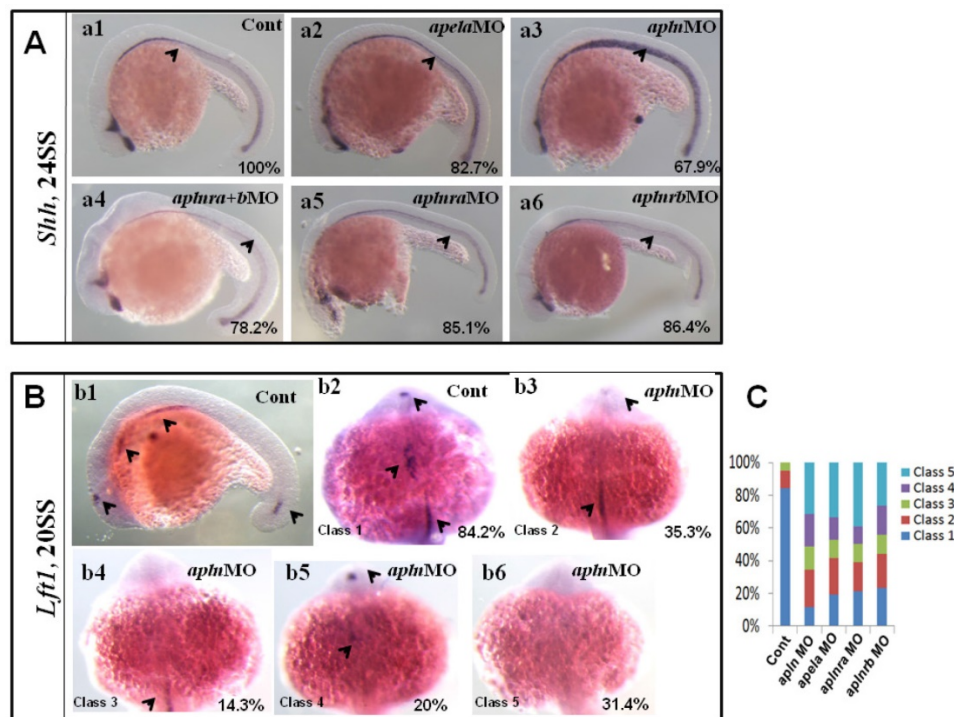


**Figure 8. Expression of midline related genes in different treated embryos.** (A. a1-a6) *Shh* expression at 24SS. Compared with that in control embryos (A. a1, 100%, n=31), no clearly decreased or increased expression of *shh* in midline was found in *apela* morphants (A. a2, 82.7%, n=29), *aplnra+b* double morphants (A. a4, 78.2%, n=23), *aplnra* morphants (A. a5, 85.1%, n=27) and *aplnrb* morphants (A. a6, 86.4%, n=22). In *apln* morphants, the expression of *shh* was slightly increased (A. a3, 67.9%, n=28). (B. b1-b6, C) Expression of *lft1* at 20SS. In wild type embryos *lft1* was expressed in 4 domains, including left telencephalon, left heart field, trunk midline and tail midline (B. b1, black arrow head, n=45), and in dorsal view, *lft1* was found to be expressed in left telencephalon, left heart field, trunk midline (B. b2, black arrow head). In *apln* morphants, *lft1* expression was found to be decreased with different phenotypes (B. b3-b6, n=85). Among all the *apln* morphants, *lft1* in midline was disappeared or decreased greatly in more than half of embryos (B. b4-b6, class 3 to class 5; C, the second column, 64.7%, n=85, p<0.01). The expression pattern of *lft1* in *apln* morphants was also found in *apela* morphants (C, column 3, 58.2%, n=79, p<0.01), *aplnra* morphants (C, column 4, 60%, n=75, p<0.01) and *aplnrb* morphants (C, column 5, 56.2%, n=89, p<0.01), near or more than half of embryos showed greatly decreased *lft1* in the trunk midline.

## Conclusion

Zebrafish G protein-coupled receptors *aplnra* /*aplnrb* were involved in organ LR patterning via an *apela/apln* ligand-dependent pathway. At the gastrulation and early somite stages, *aplnra* but not *aplnrb* was specifically involved in regulating KV/Cilia morphogenesis, coupled by the early ligand *apela* but not ligand *apln*. Thereafter, *aplnra* continued to regulate midline function by specifically regulating *lft1* expression in the trunk midline, and this role also depended on the role of the ligands *apela/apln*. Although *aplnrb* was not involved in KV/cilia morphogenesis during the gastrulation stage, at the somite stage, *aplnrb* regulated *lft1* expression in the trunk midline, left-sided *spaw* and *lft2* expression in the LPM, and subsequent organ laterality in an *apela/apln*-dependent manner. Mechanistically, at the gastrulation and early somite stages, *foxj1a* potentially lies downstream of the *Apela-Aplnra* cascade to regulate KV morphogenesis and ciliogenesis. In summary, being coupled with the endogenous ligands *apela* and *apln*, *aplnr/b* sequentially orchestrates organ LR patterning in a KV/cilia-dependent and -independent manner at different stages.

## Experimental procedures

### Ethics statement

All the experimental protocols were approved by Chengdu Medical College (Sichuan, China) and QMRC, University of Edinburgh. Zebrafish were maintained in accordance with the Guidelines of Experimental Animal Welfare from Ministry of Science and Technology of People's Republic of China (2006) and the Guidelines of Experimental Animal Welfare from Home office in UK.

### Zebrafish

Zebrafish (*Danio rerio*) of the AB genetic background (wild type), *Tg(fabp10:GFP)* (57) and *Tg(cmlc2:GFP)* (58) lines were raised and maintained at 28.5 °C, and staged by hours post-fertilization (hpf) by using morphological criteria (59).

### Morpholino and mRNA injections

The standard control MO (5'-CCTCTTACCTCA GTTACAATTTATA-3') and the following antisense morpholinos (MOs) were synthesized (Gene Tools) and applied to knock down *aplnra* (*aplnra* MO, 5'-TGTATTCCGACGTTGGCTCCATTG-3', 400 uM) (13); *aplnrb* (*aplnrb* MO, 5'-CAGAGAAGTTGTTTGTC ATGTGCTC -3', 500uM, or 100uM for low concentration) (13, 18), *apela* (*apela* MO, 5'-TGGAAGAATCTCA TGGTGATGCTCA-3', 200uM) and *apln* (*apln* MO, 5'-AACAGCCGTCACGCTCCCGACTTAC-3', 300 uM)

(13), the plasmids used for synthesizing *apela* mRNA and *apln* mRNA were gifts from Ian C Scott lab. *aplnra* mRNA, *aplnrb* mRNA, *apela* mRNA and *apln* mRNA were synthesized *in vitro* using mMESSAGE mMACHINE Kit (AM1340, Ambion). The concentration for mRNA injection was as the following: *aplnra* mRNA (for rescue experiment), 20ng/ul; *apln* mRNA, 50ng/ul; *apela* mRNA, 50ng/ul; *foxj1a* mRNA, 10ng/ul. All the MOs or mRNAs were injected at 1-4 cell stage to downregulate the expression of target genes or to rescue/overexpress the target genes in whole embryos. For specific knockdown for the target genes (*aplnra* or *apela*) in DFCs, the MO was injected into the yolk at 256-512 cell stage.

### Whole Mount In Situ Hybridization (WISH)

Whole Mount *In Situ* Hybridization (WISH) was performed according to the established methods (38) using the established antisense probe *otx5*, *apela*, *aplnrb*, *aplnra*, *apln*, *spaw*, *sox17*, *lft1*, *lft2*, *shh*, *fgf8* and *erm* (12, 13, 25, 60). To prepare the antisense probe of *cp*, *foxj1a*, *vox*, *sox32*, *vmhc* and *dnh9*, we applied the cDNA (prepared from day 3 embryos and 10 hpf embryos) to amplify the template by PCR, then synthesized the antisense probe according to the Kit manual. The embryos for *in situ* experiments were dechorionated and fixed in 4% PFA overnight at 4 °C, then washed with PBT (PBS-Tween, 0.1%), dehydrated with MeOH(100%) and stored in MeOH at -20 °C at least for 24 hours.

### Antibody staining

The embryos were fixed in 4% PFA at 4 °C for overnight and then washed with PBST (5 minutes/ times, 3 times) and 100% methanol 3 times, stored at -20 °C for at least overnight. Embryos were incubated with antibodies against alpha-tubulin (1:300; Sigma, 6793), then incubated at 4 °C overnight with Alexa fluorescent-conjugated secondary antibodies (1:1000; Invitrogen) which was diluted in the blocking solution. After washed with the PBST, embryos were proceeded for mounting and imaging.

### Quantitative PCR (Q-PCR)

The cDNA template synthesis was performed *in vitro* using RT kit (Fermantas). Quantitative PCRs were performed for *fgf8*, *erm* and *foxj1a*. The following primers were used: *fgf8* (5-GAGGCTATAAACATGA GACTCATAAC-3, 5-CGAACTCGACTCCCAAATGTG TC-3); *erm* (5-GTGAGAAGCAAGCGACATGGATG-3, 5-GAGTCTCTGCTCTTGTCCACATG-3), *foxj1a* (5-CTATCGAGGAAGGACAGGATTTG-3, 5- GTCAGT GGCATGCCTATAGACGC -3). *mxtx2* (5-CAGCACA ATGGCAGTCGTGCAC-3; 5-CTTTCTCCAGCACGT CGATCIG-3); *ndnr2*(5-CTTGCTACTGCCAGCTGCT G-3; 5-CAGTGCTGTGTTACGCTCAGCAG-3), *sox32*

(5-CAGCATGTATCTCGACCGGATG-3; 5-CGICTTACTCGAGTTTCCACG-3) and *ism1* (5-GTGAAGAGGATGGTTCGTCTGG-3; 5-GAATATGAGCCACCCGAGTCTG-3). Transcription of *beta-actin* (5-CATGGATGAGGAAATCGCTGCC-3, 5-GCTCAGGATACCTCTCTTGCTC-3) was used for normalization.

### SgRNAs preparing and Cas9 protein co-injection

Four sgRNAs for *aplnra*, *apln* and *apela* were designed according to previous report (61). The individual sgRNA templates for each gene were prepared and then pooled to synthesize the sgRNAs *in vitro* (NEB #E2040S). The prepared sgRNAs were mixed with Cas9 protein (NEB, #M0646T) (The final concentration for sgRNAs and Cas9 protein were 4μM and 600ng/ul, respectively), and co-injected into the cytoplasm at the one cell stage. For one pool of embryos injected, part of the injected embryos were raised to 27 hpf for analyzing whether the heart cells were decreased greatly, and part of the sorted embryos were used to check genome editing efficiency using PCR. While the remaining embryos injected were raised to stages needed for LR asymmetric phenotype analysis. The sgRNAs targeted for each genes were as: *aplnra* sgRNA1: ACGGGAATGAGAGTAAGA, *aplnra* sgRNA2: TTTCCAAATGGA GCCAACGT, *aplnra* sgRNA3: CGCCGTTCCCGGACAAACCG, *aplnra* sgRNA4: TGTGGCGCGGAAATC AAA; *apln* sgRNA1: CTGGGGAGAGGAGGGAAA, *apln* sgRNA2: GACTGGCAGGGAAACGGA, *apln* sgRNA3: CGCTGGTGATTGTGCTGG, *apln* sgRNA4: AGCGTGACGGCTGTTGCC; *apela* sgRNA1: AGCAGCAGATACAGCGGG, *apela* sgRNA2: CAGCAGCAGCAGATACAG, *apela* sgRNA3: AGACTCGACTCTCC TCAC, *apela* sgRNA4: GTGATGCTCAGGGTGGTT. The specific primers for checking genome editing efficiency were as the following: *aplnra*\_F: 5\_CTGCTC AAGAAGGACTCAAAGCC\_3, *aplnra*\_R: 5\_GTGGAC GATGGCGAGGTAG\_3; *apln*\_F: 5\_CGCACTGAAGA GCAAACAGTC\_3, *apln*\_R: 5\_CATGCAGAAGTCGG CAAGTAATT\_3; *apela*\_F: 5\_GGATTTCTACAGTCC GTTAC\_3, *apela*\_R: 5\_CTCGAATCGTTTGCCTCAT G\_3.

### Microscope

To examine the KV morphogenesis, the heart and liver of the living embryos in transgenic lines, the embryos were laid in the proper holes made in the Agar plate (1.5% of Low Melting-point Agar (LMP, Sigma)) or directly laid on the Agar plate. *In situ* hybridized, immunostained embryos were mounted in the 100% glycerol for imaging. Images for living embryos and for *in situ* experiments were captured at room temperature using AxioVision4 software (Carl

Zeiss, Inc.). Cilia images were captured by using LAS AF software (Leica), a x20/0.70 N.A. HC Plan Apochromat air objective (Leica).

### Abbreviations

hpf: hours post fertilization; dpf: days post-fertilization; WISH: whole-mount *in situ* hybridization; qPCR: quantitative PCR; LR patterning: left-right patterning; GPCP: G protein coupled receptor; MPCs: myocardial progenitor cells; DFCs: dorsal forerunner cells; KV: Kupffer's vesicle; LPM: lateral plate mesoderm; KO: Knock Out.

### Supplementary Material

Supplementary figures.

<http://www.ijbs.com/v15p1225s1.pdf>

### Acknowledgements

We are most grateful to Dr. Yi Feng's lab to host most of this work in University of Edinburgh, and to the members in Yi Feng's lab. We are also grateful to Dr. Ian C Scott and Dr. Qiang Wang for the gift plasmids.

### Author contributions statement

S.H, C.Z, Z.G designed the experiments. C.Z, Y.Z, M.L, ZG, and S.H performed the experiments, K.C, Y.W, M.Y, X.Z, H.Z, H.T, M. L, C. L, B. S, Y. F, S. L and X.Y discussed the results and commented on the manuscript, S.H, C.Z, Z.G, F.Y, Y.W wrote the manuscript.

### Funding

This work was supported by the National Key Research and Development Program of China (2017YFA0106600), National Natural Science Foundation of China (No. 31741091, 31470080, 31201092, 81573154, 81773432), Royal Society K.C. Wong Foundation (NF140476) and Scientific Research Fund of Sichuan Provincial Education Department (18Z021).

### Competing Interests

The authors have declared that no competing interest exists.

### References

- O'Dowd BF, Heiber M, Chan A, et al. A human gene that shows identity with the gene encoding the angiotensin receptor is located on chromosome 11. *Gene*. 1993; 136:355-360.
- Tatemoto K, Hosoya M, Habata Y, et al. Isolation and characterization of a novel endogenous peptide ligand for the human APJ receptor. *Biochem Biophys Res Commun*. 1998; 251: 471-476.
- Charo DN, Ho M, Fajardo G, et al. Endogenous regulation of cardiovascular function by apelin-APJ. *Am J Physiol Heart Circ Physiol*. 2009; 297: H1904-1913.
- Farkasfalvi K, Stagg MA, Coppen SR, et al. Direct effects of apelin on cardiomyocyte contractility and electrophysiology. *Biochem Biophys Res Commun*. 2007; 357: 889-895.

5. Kuba K, Zhang L, Imai Y, et al. Impaired heart contractility in Apelin gene-deficient mice associated with aging and pressure overload. *Circ Res.* 2007; 101: e32-42.
6. Sonmez A, Celebi G, Erdem G, et al. Plasma apelin and ADMA Levels in patients with essential hypertension. *Clin Exp Hypertens.* 2010; 32: 179-183.
7. D'Aniello C, Lonardo E, Iaconis S, et al. G protein-coupled receptor APJ and its ligand apelin act downstream of Cripto to specify embryonic stem cells toward the cardiac lineage through extracellular signal-regulated kinase/p70S6 kinase signaling pathway. *Circ Res.* 2009; 105: 231-238.
8. Pitkin SL, Maguire JJ, Kuc RE, et al. Modulation of the apelin/APJ system in heart failure and atherosclerosis in man. *Br J Pharmacol.* 2010; 160: 1785-1795.
9. Hashimoto T, Kihara M, Imai N, et al. Requirement of apelin-apelin receptor system for oxidative stress-linked atherosclerosis. *Am J Pathol.* 2007; 171: 1705-1712.
10. Chun HJ, Ali ZA, Kojima Y, et al. Apelin signaling antagonizes Ang II effects in mouse models of atherosclerosis. *J Clin Invest.* 2008; 118: 3343-3354.
11. Tucker B, Hepperle C, Kortschak D, et al. Zebrafish Angiotensin II Receptor-like 1a (agtr1a) is expressed in migrating hypoblast, vasculature, and in multiple embryonic epithelia. *Gene Expr Patterns.* 2007; 7: 258-265.
12. Chng SC, Ho L, Tian J, et al. ELABELA: a hormone essential for heart development signals via the apelin receptor. *Dev Cell.* 2013; 27: 672-680.
13. Scott I C, Masri B, D'Amico LA, et al. The g protein-coupled receptor agtr1b regulates early development of myocardial progenitors. *Dev Cell.* 2007; 12: 403-413.
14. Pauli A, Norris ML, Valen E, et al. Toddler: an embryonic signal that promotes cell movement via Apelin receptors. *Science* 2014;343: 1248636.
15. Nornes S, Tucker B, and Lardelli M. Zebrafish aplnra functions in epiboly. *BMC Res Notes.* 2009; 2: 231
16. Deshwar AR, Chng SC, Ho L, et al. The Apelin receptor enhances Nodal/TGFbeta signaling to ensure proper cardiac development. *Elife.* 2016; 5.
17. Paskaradevan S, Scott IC. The Aplnr GPCR regulates myocardial progenitor development via a novel cell-non-autonomous, Galpha(i/o) protein-independent pathway. *Biol Open.* 2012; 1: 275-285.
18. Zeng XX, Wilm TP, Sepich DS, et al. Apelin and its receptor control heart field formation during zebrafish gastrulation. *Dev Cell.* 2007; 12: 391-402.
19. Kim JD, Kang Y, Kim J, et al. Essential role of Apelin signaling during lymphatic development in zebrafish. *Arterioscler Thromb Vasc Biol.* 2014; 34: 338-345.
20. Karpinich NO, Caron KM. Apelin signaling: new G protein-coupled receptor pathway in lymphatic vascular development. *Arterioscler Thromb Vasc Biol.* 2014; 34: 239-241.
21. Kang Y, Kim J, Anderson JP, et al. Apelin-APJ signaling is a critical regulator of endothelial MEF2 activation in cardiovascular development. *Circ Res.* 2013; 113: 22-31.
22. Speder P, Petzoldt A, Suzanne M, et al. Strategies to establish left/right asymmetry in vertebrates and invertebrates. *Curr Opin Genet Dev.* 2007; 17: 351-358.
23. Raya A, Izpisua Belmonte JC. Left-right asymmetry in the vertebrate embryo: from early information to higher-level integration. *Nat Rev Genet.* 2006; 7: 283-293.
24. Long S, Ahmad N, Rebagliati M. The zebrafish nodal-related gene southpaw is required for visceral and diencephalic left-right asymmetry. *Development.* 2003; 130: 2303-2316.
25. Huang S, Ma J, Liu X, et al. Geminin is required for left-right patterning through regulating Kupffer's vesicle formation and ciliogenesis in zebrafish. *Biochem Biophys Res Commun.* 2011; 410: 164-169.
26. Essner JJ, Amack JD, Nyholm MK, et al. Kupffer's vesicle is a ciliated organ of asymmetry in the zebrafish embryo that initiates left-right development of the brain, heart and gut. *Development.* 2005; 132: 1247-1260.
27. Wang G, Cadwallader AB, Jang DS, et al. The Rho kinase Rock2b establishes anteroposterior asymmetry of the ciliated Kupffer's vesicle in zebrafish. *Development.* 2011; 138: 45-54.
28. Caron A, Xu X, Lin X. Wnt/beta-catenin signaling directly regulates Foxj1 expression and ciliogenesis in zebrafish Kupffer's vesicle. *Development.* 2012; 139: 514-524.
29. Lai SL, Yao WL, Tsao KC, et al. Autotaxin/Lpar3 signaling regulates Kupffer's vesicle formation and left-right asymmetry in zebrafish. *Development.* 2012; 139: 4439-4448.
30. Manning DK, Sergeev M, van Heesbeen RG, et al. Loss of the ciliary kinase Nek8 causes left-right asymmetry defects. *J Am Soc Nephrol.* 2013; 24: 100-112.
31. John LB, Trengove MC, Fraser FW, et al. Pegasus, the 'atypical' Ikaros family member, influences left-right asymmetry and regulates pitx2 expression. *Dev Biol.* 2013; 377: 46-54.
32. Ellertsdottir E, Ganz J, Durr K, et al. A mutation in the zebrafish Na,K-ATPase subunit atp1a1a.1 provides genetic evidence that the sodium potassium pump contributes to left-right asymmetry downstream or in parallel to nodal flow. *Dev Dyn.* 2006; 235: 1794-1808.
33. Helker CS, Schuermann A, Pollmann C, et al. The hormonal peptide Elabela guides angioblasts to the midline during vasculogenesis. *Elife.* 2015; 4.
34. Liu J, Zhou Y, Qi X, et al. CRISPR/Cas9 in zebrafish: an efficient combination for human genetic diseases modeling. *Hum Genet.* 2017; 136: 1-12.
35. Wu R S, Lam II, Clay H, et al. A Rapid Method for Directed Gene Knockout for Screening in G0 Zebrafish. *Dev Cell.* 2018; 46: 112-125 e114.
36. Shankaran SS, Dahlem TJ, Bisgrove BW, et al. CRISPR/Cas9-Directed Gene Editing for the Generation of Loss-of-Function Mutants in High-Throughput Zebrafish F0 Screens. *Curr Protoc Mol Biol.* 2017; 119: 31.9.1-31.9.22.
37. Norris ML, Pauli A, Gagnon JA, et al. Toddler signaling regulates mesodermal cell migration downstream of Nodal signaling. *Elife.* 2017; 6.
38. Huang S, Ma J, Liu X, Zhang Y, et al. Retinoic acid signaling sequentially controls visceral and heart laterality in zebrafish. *J Biol Chem.* 2011; 286: 28533-28543.
39. O'Carroll AM, Lolait SJ, Harris LE, et al. The apelin receptor APJ: journey from an orphan to a multifaceted regulator of homeostasis. *J Endocrinol.* 2013; 219: R13-35.
40. Yang P, Read C, Kuc RE, et al. Elabela/Toddler Is an Endogenous Agonist of the Apelin APJ Receptor in the Adult Cardiovascular System, and Exogenous Administration of the Peptide Compensates for the Downregulation of Its Expression in Pulmonary Arterial Hypertension. *Circulation.* 2017; 135: 1160-1173.
41. Roberts EM, Newson MJ, Pope GR, et al. Abnormal fluid homeostasis in apelin receptor knockout mice. *J Endocrinol.* 2009; 202: 453-462.
42. Tay HG, Schulze SK, Compagnon J, et al. Lethal giant larvae 2 regulates development of the ciliated organ Kupffer's vesicle. *Development.* 2013; 140:1550-1559.
43. Dasgupta A, Merkel M, Clark MJ, et al. Cell volume changes contribute to epithelial morphogenesis in zebrafish Kupffer's vesicle. *Elife.* 2018; 7.
44. Neugebauer JM, Amack JD, Peterson AG, et al. FGF signalling during embryo development regulates cilia length in diverse epithelia. *Nature.* 2009; 458: 651-654.
45. Matsui T, Thitamadee S, Murata T, et al. Canopy1, a positive feedback regulator of FGF signaling, controls progenitor cell clustering during Kupffer's vesicle organogenesis. *Proc Natl Acad Sci U S A.* 2011; 108: 9881-9886.
46. Aquilina-Beck A, Ilagan K, Liu Q, et al. Nodal signaling is required for closure of the anterior neural tube in zebrafish. *BMC Dev Biol.* 2007; 7: 126.
47. Frisca F, Colquhoun D, Goldshmit Y, et al. Role of ectonucleotide pyrophosphatase/phosphodiesterase 2 in the midline axis formation of zebrafish. *Sci Rep.* 2016; 6: 37678.
48. Burdine RD, Grimes DT. Antagonistic interactions in the zebrafish midline prior to the emergence of asymmetric gene expression are important for left-right patterning. *Philos Trans R Soc Lond B Biol Sci.* 2016; 371:1710
49. Xu J, Chen L, Jiang Z, et al. Biological functions of Elabela, a novel endogenous ligand of APJ receptor. *J Cell Physiol.* 2018. 9:6472-6482
50. Szokodi I, Tavi P, Foldes G, et al. Apelin, the novel endogenous ligand of the orphan receptor APJ, regulates cardiac contractility. *Circ Res.* 2002; 91: 434-440.
51. Huang S, Xu W, Su B, et al. Distinct mechanisms determine organ left-right asymmetry patterning in an uncoupled way. *Bioessays.* 2014; 36: 293-304.
52. Roxo-Rosa M, Jacinto R, Sampaio P, et al. The zebrafish Kupffer's vesicle as a model system for the molecular mechanisms by which the lack of Polycystin-2 leads to stimulation of CFTR. *Biol Open.* 2015; 4: 1356-1366.
53. Zhang J, Jiang Z, Liu X, et al. Eph/ephrin signaling maintains the boundary of dorsal forerunner cell cluster during morphogenesis of the zebrafish embryonic left-right organizer. *Development.* 2016; 143: 2603-2615.
54. Gokey JJ, Ji Y, Tay HG, et al. Kupffer's vesicle size threshold for robust left-right patterning of the zebrafish embryo. *Dev Dyn.* 2016; 245: 22-33.
55. Dasgupta A, Amack JD. Cilia in vertebrate left-right patterning. *Philos Trans R Soc Lond B Biol Sci.* 2016; 371.
56. Matsui T, Bessho Y. Left-right asymmetry in zebrafish. *Cell Mol Life Sci.* 2012; 69: 3069-3077.
57. Lu H, Ma J, Yang Y, et al. EpCAM is an endoderm-specific Wnt derepressor that licenses hepatic development. *Dev Cell.* 2013; 24: 543-553.
58. Huang CJ, Tu CT, Hsiao CD, et al. Germ-line transmission of a myocardium-specific GFP transgene reveals critical regulatory elements in the cardiac myosin light chain 2 promoter of zebrafish. *Dev Dyn.* 2003; 228: 30-40.
59. Kimmel CB, Ballard WW, Kimmel SR, et al. Stages of embryonic development of the zebrafish. *Dev Dyn.* 1995; 203: 253-310.
60. Carl M, Bianco IH, Bajoghli B, et al. Wnt/Axin1/beta-catenin signaling regulates asymmetric nodal activation, elaboration, and concordance of CNS asymmetries. *Neuron.* 2007; 55: 393-405.
61. Varshney GK, Pei W, LaFave MC, et al. High-throughput gene targeting and phenotyping in zebrafish using CRISPR/Cas9. *Genome Res.* 2015; 25: 1030-1042